Ocean Research 22(2): 81-90, 2000

Simplified Numerical Model of the Wind-driven Circulation with Emphasis on Distribution of the Tuman River Solid Run-off

N.S. Vanin, A.V. Moshchenko*, K.L. Feldman*, G.I. Yurasov+

V.I.Il'ychev Pacific Oceanological Institute, Far East Branch, Russian Academy of Sciences, 43 Baltiyskaya St., Vladivostok 690041, Russia

**Institute of Marine Biology, Far East Branch, Russian Academy of Sciences, 17 Palchevskogo St., Vladivostok 690041, Russia*

Abstract: Supposed construction of a large port in the mouth of Tuman River requires careful examination of possible unfavorable ecological consequences for the Far Eastern Federal Marine Reserve. Since the Tuman River is the largest source of suspended material and possible contaminants flowing into the sea, and in order to understand how this material is allocated in the coastal zone, analyses are needed to check possible pathways of water transport and circulation system in the region. Linearized shallow water equations were used for numerical simulation of the wind-driven circulation to the north off the Tuman River mouth. The model results satisfactorily agreed with *in situ* data. The model circulation patterns are largely dependent on the wind direction and are confirmed by the distribution of bottom sediments, and by the location of organic carbon and some pollutants accumulation zones. The most unfavorable situation for the Marine Reserve is the case of the southwesterly wind; even with quite moderate wind, the waters polluted by the run-off from the Tuman River can attain the south section of the Marine Reserve during the diurnal period.

Key words: Numerical simulation, Wind-driven circulation, Shallow water equations.

1. Introduction

In connection with the presumably intense economical exploitation of the region situated closely to the territory of the Far Eastern Federal Marine Reserve (Fig.1), and its possibly unfavorable environmental consequences, the current system as a main mechanism of suspensions and pollutants transport should be carefully examined. Since the instrumental observations have revealed occasional patterns, they do not completely reflect the system of circulation. Intricate bottom relief and coastline, tidal and storm surge events also make a contribution to variability of the local circulation.

In recent years, the Institute of Marine Biology has conducted extended environmental investigations in the region of the Marine Reserve. An intensive sedimentation (mud accumulation) was discovered in the central part of the region (Moshchenko *et al.* 1999a, 1999b, 2000, 2001b). It threatens the ecological system of the Reserve. The main source of contamination in the region is the Tuman River run-off (Moshchenko *et al.* 2001a; Shulkin and Moshchenko 2000); therefore, it is the main motivation for this study to understand how the suspended material and contaminants move and accumulate in the Reserve.

+Corresponding author.
E-mail : pacific@online.marine.su

Instrumental observations revealed that the circulation system is influenced mainly by the wind impact and tidal oscillations (Grigorieva and Moshchenko 1998).

Tidal fluctuations have an irregular semi-diurnal pattern and their amplitudes do not exceed 50 cm (Lastovetskiy and Yakunin 1981). Thus their influence is pronounced only during the periods of weak winds (less then 5 m/s), and their action is particularly noticeable in the southern part of the region near the mouth of Tuman River. The general tidal transport has oscillatory character; during flood phase, the current is directed northward, and during ebb phase, is directed south to southwestward (Grigorieva and Moshchenko 1998). Velocities of the tidal currents in the southern part can reach up to 20-40 cm/s and 3-8 cm/s in the northern part.

Research area is located in the open coastal region directly affected by seasonally varying wind impact. During winter, the northwesterly winds caused by the Siberian anticyclone and blowing through the Khanka Valley promote intense cooling and mixing of the coastal waters. In warm period, the southeasterly winds prevail due to the interaction of the Asian Low and the North Pacific High. Total recurrence of the northwesterly and southeasterly winds reaches up to 90% (Lastovetskiy and Yakunin 1981). It seems reasonable to check the wind-driven circulation patterns for main wind directions, since in definite conditions the wind impact may be prevailing (Grigorieva and Moshchenko 1998).

2. Numerical Model

The depths in the research area usually do not exceed 30-50 m, excluding the south and southeast parts, where the depths are greater than 500 m. Thus the wind impact at the most part of the region can penetrate whole water columns to the seabed. The equations to be solved are vertically integrated and linearized momentum and continuity equations for a homogenous fluid with surface and bottom stresses (Volcinger and Pyaskovskii 1977; Beardsley and Haidvogel 1981; Chapman 1985):

$$\frac{\partial u}{\partial t} = fv - g\frac{\partial \xi}{\partial x} + \frac{\tau_x^s - \tau_x^b}{\rho_w H} \quad (1)$$

$$\frac{\partial v}{\partial t} = -fu - g\frac{\partial \xi}{\partial y} + \frac{\tau_y^s - \tau_y^b}{\rho_w H} \quad (2)$$

$$\frac{\partial \xi}{\partial t} + \frac{\partial (uH)}{\partial x} + \frac{\partial (vH)}{\partial y} = 0 \quad (3)$$

where u and v are the components of vertically averaged current velocity along the X and Y axes, respectively; t is the time; ξ is the elevation of the sea surface above its mean level; $f = 2\omega \sin\varphi$ is the Coriolis' parameter (ω is the angular velocity of the earth rotation, φ is latitude); $H = \xi + R$ is the total sea depth (R is still water depth); ρ_w is the sea water density (assumed to be constant as 1.02); g is the acceleration due to the gravity; τ_x^s and τ_y^s are the components of the tangential wind stress at the sea surface; τ_x^b and τ_y^b are the components of bottom stress.

At the sea surface and seabed, a quadratic friction law is applied, thus

$$\tau_x^s = \rho_a \lambda W_x \sqrt{W_x^2 + W_y^2}, \quad \tau_y^s = \rho_a \lambda W_y \sqrt{W_x^2 + W_y^2} \quad (4)$$

$$\tau_x^b = \rho_w r u \sqrt{u^2 + v^2}, \quad \tau_y^b = \rho_w r v \sqrt{u^2 + v^2} \quad (5)$$

where ρ_a is the air density; λ is the coefficient of surface friction; W_x and W_y are the components of the wind velocity, r is the coefficient of bottom friction. Surface and bottom friction coefficients are chosen as 3.2×10^{-3} and 2.6×10^{-3}, respectively (Duun-Christiansen 1975; Henry and Heaps 1976; Saveliev 1989).

The region studied represents a rectangle of 29×35 km in the X and Y axes, respectively. X axis is oriented eastward and Y axis northward. The beginning of coordinates is located at the point of 42° 14' N and 130° 38' E. The grid interval of the model was chosen as 1 km. The relation between time and space steps was determined according to the stability condition of the Courant-Friedrichs-Lewy (CFL) numerical scheme (Duun-Christiansen 1975):

$$2\tau \le 2h / \sqrt{2gH_{max}} \quad (6)$$

where h is the value of the grid interval in meters, H_{max} is the maximal depth of the research area.

Numerical approximation of the equations (1)-(3) was carried out by the HN-method elaborated by Hansen (1961) using the explicit scheme with central differences for space and time derivatives. On the land boundaries,

no normal flux condition was accepted. In order to remove the wave reflection along the open boundaries, we used the radiation condition, given by:

$$\xi_{x1} = -v\sqrt{H_{g1}/g}\,,\ \xi_{x2} = v\sqrt{H_{g2}/g} \qquad (7)$$

where ξ_{x1} and ξ_{x2} are the deviations of sea level from undisturbed state at the east, north and south boundaries; H_{g1} and H_{g2} are the values of total depth in the nodes of grid field along these boundaries, respectively. Such approach was successfully used for modeling of the wind-induced currents at the shelf of Sakhalin Island and in Anadyr Bay (Menovshchikov and Saveliev 1989; Saveliev 1989).

Influence of the boundary conditions for barotropic coastal model with uniform cross-shelf slope is investigated by Chapman (Chapman 1985). He has shown the importance of the open boundary condition depending on whether. Wind is blowing along the shelf or shelf crossing. In our case, as it is shown below, due to boundary conditions (7), unrealistic current velocities occur in the southeastern part of the region, where a sharp depth slope is observed. Water depths in the nodes of the grid field were obtained by interpolation of the depths withdrawn from the navigation map and added by depths taken from the stationary net of hydrological stations in the research area (Fig. 1).

During field investigations in July-September 1996 and July-October 1997, the frequencies of each wind direction exceeded 10% (Fig. 2). Directions and velocities of the wind used in the simulation were chosen according to the most frequent observtions made during the study period in 1996-1997: 110-120°, 8 m/s; 70-80°, 7 m/s; 225°, 5 and 10 m/s; 315°, 10 m/s; 360°, 10 m/s. In addition, we simulated currents under the typical winter and summer storm conditions; wind directions of 0° and 135° with the velocity of 20 m/s. Considering the small size of the study region the wind can be assumed to be spatially uniform in all cases.

In the initial state, the sea level and velocity components were set to zero. According to the CFL stability condition, a time step of 5 seconds was used for calculations. The model was started from an initial state and integrated forward in time until the sea level in control points became invariable with specified accuracy. For different wind cases, it took 6 to 8 hours to reach stability.

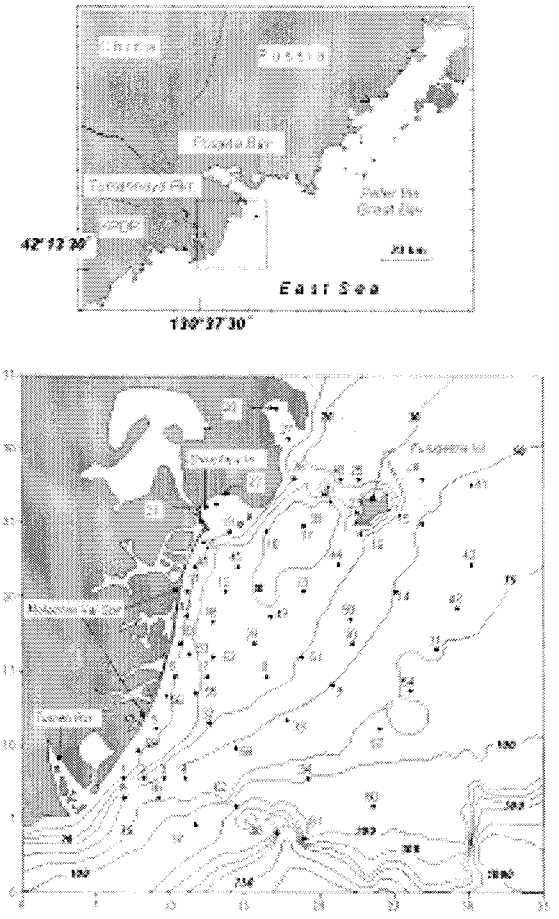

Fig. 1. Map of the research area. Closed circles are the locations of the hydrological stations with their numbers. Dotted line shows the Far Eastern Federal Marine Reserve boundaries. Axes are distances in km from the point with coordinates of 42°14' N, 130°38' E.

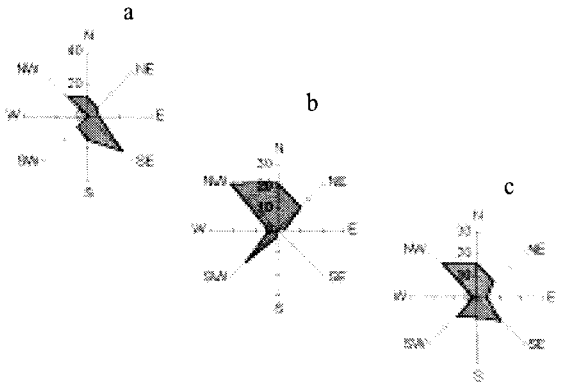

Fig. 2. Frequencies (%) of wind directions in the region during the study period of 1996-1997. (a) summer (July-August), (b) autumn (September-October) and (c) average (July-October).

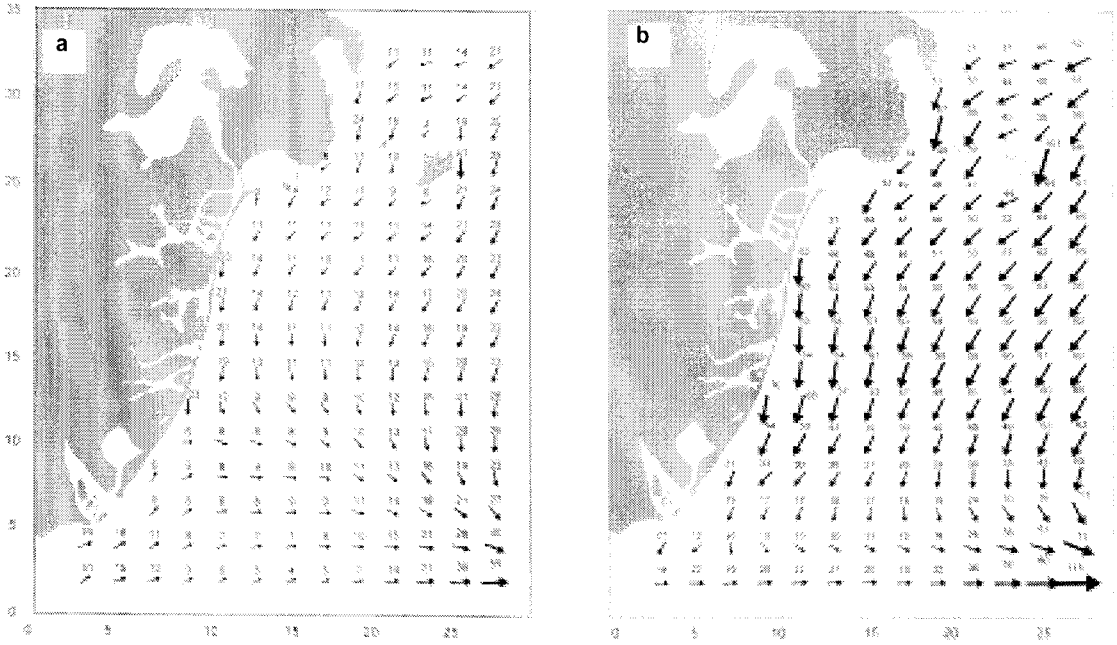

Fig. 3. Circulation patterns with current speed (cm/s) during (a) weak (5 m/s) and (b) stormy (20 m/s) northerly winds.

3. Results and Discussion

The calculation results of the wind-driven circulation in the research area are shown on Figs. 3-5. Under the action of weak northerly winds (up to 5 m/s) the general flow in the main part of the region is oriented to the southwest along the coast, and only near the depth slope in the southern part of the region, it turns eastward (Fig.3(a)). The model current velocities in the northern and central parts of the region, during such winds reach up to 10-15 cm/s, and increase to the south up to 30-50 cm/s. With the wind velocity rising up to storm condition, the circulation pattern does not change, but the current velocity increases up to 50-60 cm/s in the central part of the region, and up to 70-100 cm/s at the southeastern part (Fig.3(b)). Strong currents are also observed around the Furugelma Island. The circulation pattern quoted above is generally kept during the northwesterly and northeasterly winds (315-75°).

More complicated circulation patterns occur under the influence of the southeasterly winds, which are typical for summer monsoon season(Fig.4). During the action of moderate wind condition (8 m/s) with the direction at 115° the cyclonic gyre with the center located between isobaths of 50 and 75 m appears in the southeastern part of the region (Fig.4(a)). In the northern part of region, the anticyclonic gyre is formed over the bottom depression off Sivuchiya Inlet. Along the eastern boundary of the region, the flow is directed to the north. In the central part between the two gyres, the flow is oriented to the southwest, and along the southern boundary, it flows to the east. The maximal current velocities are seen off the eastern side of the Furugelma Island, and off the southern boundary of the region. They reach up 21 and 25-35 cm/s, respectively. With the increase of the wind speed from moderate to storm condition for the southeasterly wind, the center of cyclonic gyre shifts to south in the region of 150-200 m in depth, and the anticyclonic gyre off Sivuchiya Inlet decreases in size and nestles to the coastline. Similar to the moderate wind forcing, the main flow is directed to the southwest, and turns to the east off the southern boundary. Along the eastern boundary, the current is oriented strictly to the north, and its velocities reach up to 40 cm/s. Coming nearer to the Furugelma Island, some part of the flow turns to the west and joins to the main southwest flow moving along the axis of the seabed depression. With the rotation of the storm winds clockwise up to 135°, the cyclonic gyre shifts to the southwest and comes nearer to the mouth of Tuman River (Fig.4(b)). The main

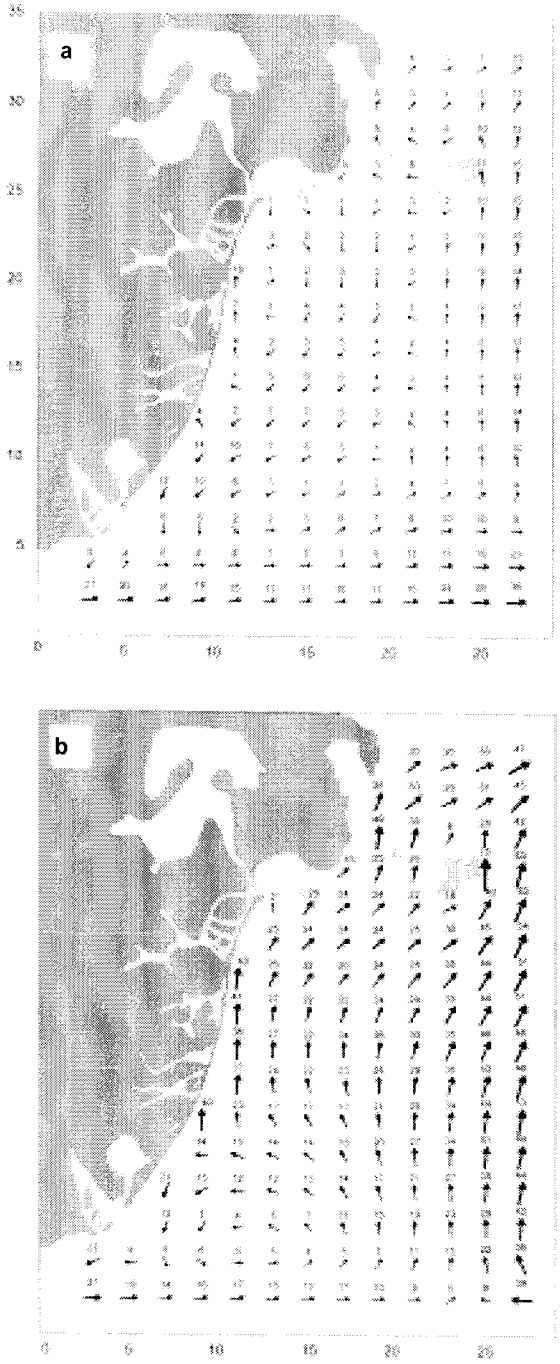

Fig. 4. Circulation patterns with current speed (cm/s) during (a) moderate (8 m/s) and (b) stormy (20 m/s) southeasterly winds.

flow to the north off the cyclonic gyre is directed along the coast to the north and northeast, and crosses the underwater crest connecting the Furugelma Island with

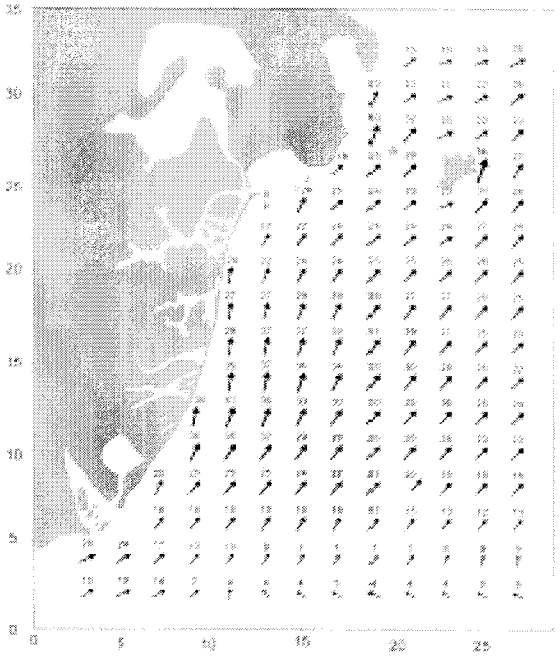

Fig. 5. Circulation pattern with current speed (cm/s) during moderate (10 m/s) southwesterly wind.

the continent. The anticyclonic circulation located to the east off Sivuchiya Inlet vanishes.

With the southwesterly winds (10 m/s) in the whole region, the northward and northeastward flows prevail, and the strong velocities are obtained in the coastal zone (35-40 cm/s), and off the eastern side of the Furugelma Island (56 cm/s). The current the strait also becomes strong as large as 40 cm/s (Fig. 5).

It is natural that the general circulation patterns with the southwesterly and northerly winds are contrary to each other. With the southerly and southwesterly wind, the main flow is directed to the north and northeast; and with the northerly wind, it is oriented to the southwest. But due to the southeasterly wind, the cyclonic circulation appears in the southern part of the region. As a result, the main flow bifurcates with one of its branches moving to the north, and another one flowing to the southwest. Another remarkable feature is that the current near the southern boundary is oriented eastward, which is independent on the wind direction(except the southwesterly winds). This is caused evidently by sharp north-south continental slope along the southern boundary, and this effect may be prevailing here. In any case,

Table 1. Results of Wilcoxon's matched pairs test for different wind conditions. Computed probabilities presented here show that there are no significant differences between observed and computed current velocities and directions during southeasterly and northeasterly winds. Boldface was used to show significant differences between observed and computed velocity values during southwesterly winds.

Parameter	Wind		
	Southeasterly	Southwesterly	Northeasterly
Current velocity	0.694	**0.039**	0.276
Current direction	0.875	0.813	0.612

the eastward current was observed here in most cases even by visually. But its velocities are 2-3 times less than those obtained in the model calculations. This difference may be caused rather by unsuccessful choice of the boundary conditions applied in the present study. But looking over various boundary conditions is not in the scope of our present work, though it may be important for this site of research area.

Reliability of the calculated current directions and velocities was estimated by comparison of these parameters with those obtained by the CM-2 current meter produced by the Toho Dentan Corp., Japan, for the residual currents at the hydrological stations (Fig. 1). For each dominant wind situation, we used the data from 15 to 25 observations of current velocity and direction obtained in July-September, 1996 and in July, 1997. The results of the Wilcoxon's matched pair test (STATISTICA for Windows, 1996) do not show any significant differences between the velocities and directions of the simulated currents and observed ones for moderate southeasterly and northeasterly wind situations (Table 1). Only for the southwesterly winds, the differences were found to be significant in current velocity; the mean observed velocity was less by 25-30%.

As a whole, to evaluate the reliability of the simulated circulation patterns, it is necessary, at least, to have long-term current observations enough to exclude tidal components, and to capture different wind situations. Since there are no other similar observations, the reliability of the circulation patterns obtained may be indirectly evaluated by the distribution of the granulometric and chemical properties of the seabed sediments. In order to trace possible ways of suspended material transportations the water pathways (Fig. 6) were calculated by integrating the velocity field with time step of 2-4 hours. Evidently, major part of fine suspended material enriched by terrigenous organic carbon and pollutants originating from the Tuman River mouth during the southeasterly winds will remain in the vicinity of the source region because of its recirculation into the cyclonic eddy. However, some part of it moves to the north and may cause the pelite accumulation in the eastern part of the basin (compare Figs. 6(b) and Fig. 7). During these wind events, the major part of suspended matters coming from Sivuchiya Inlet is deposited at the seabed in the depression and in the middle of the coastal area.

The temporary wetlands located in the middle part of the Molochnyi Val Spit are additional sources of the solid discharges. These wetlands can be opened during heavy floods. But suspended material mainly remains near their mouths due to weakening of currents caused by the stream divergence.

During the southwesterly winds, suspended material moves to the north and northeast from the Tuman River mouth and wetlands, and settles mainly in the coastal area and in the bottom depression. These winds are the most unfavorable for this depression because contaminant outbreaks from the river mouth and wetlands during flood can reach and settle down at the seabed within a day (Fig. 6(a)). But fine sediments from Sivuchiya Inlet, probably, do not have time to settle here under these wind conditions and move through the strait between the continent and Furugelma Island. They can accumulate in the local spot to the northeast off this island due to the eddy that may be formed here similar to other comparable orographic structures. However, silt accumulation in this spot may also occur under the southeasterly wind because of the transfer of suspended material by the stream flowing along the eastern boundary of the region.

Under the action of the north and northwesterly winds suspended material from the mouth is transported eastward (Fig. 6(c) and (d)). Some material coming from the north through the strait and from Sivuchiya Inlet accumulate in the depression. Some other material from the wetlands also may approach the river mouth and merge with the main flow moving to the east.

The zone with the largest mean granule sizes and with the most well sorted sediments is situated in the offshore central part of the region studied (Fig. 7). Large granule sizes show the higher stress level of hydrodynamic sedimentogenesis here than in other parts of the region, and

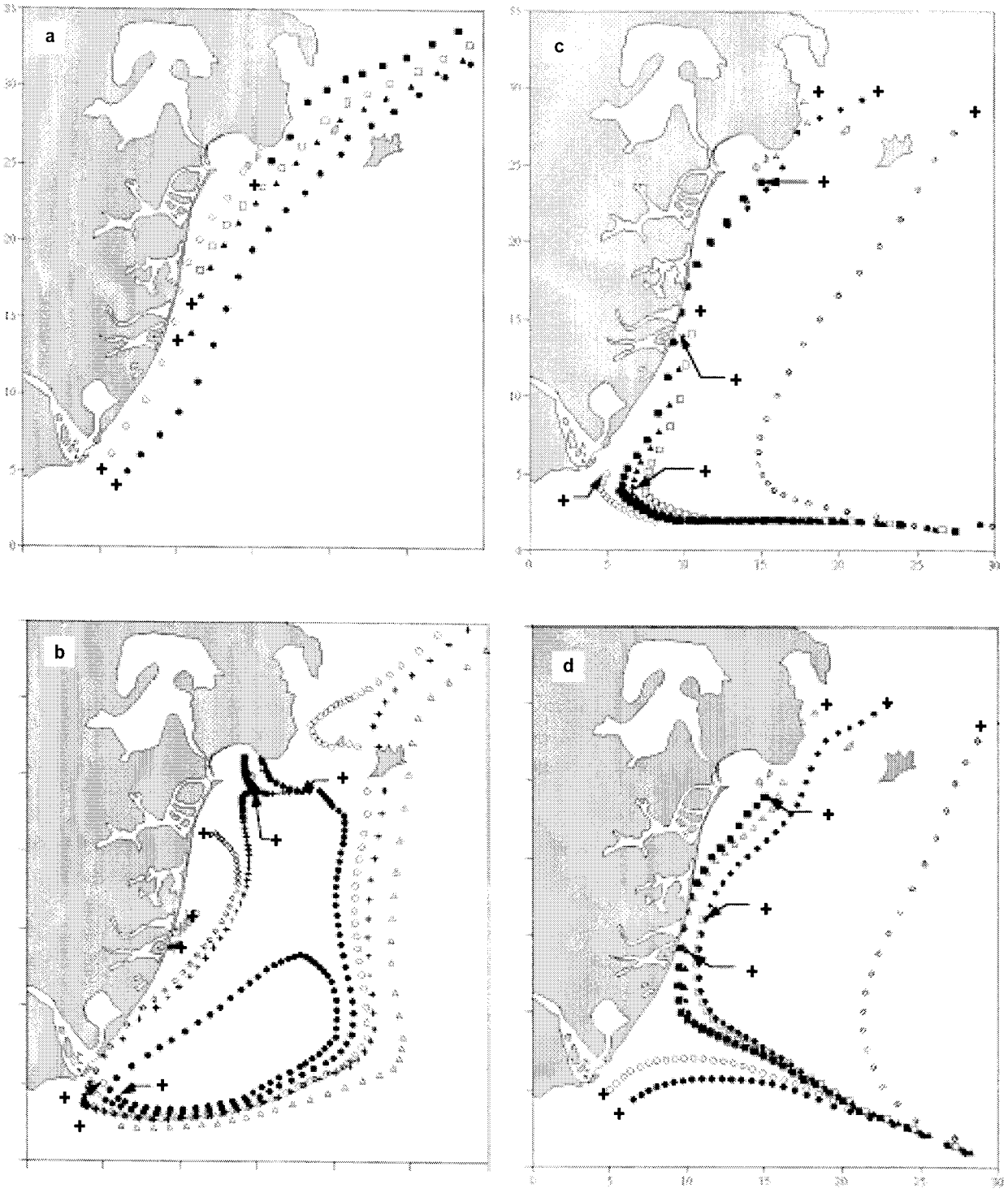

Fig. 6. Water pathways under the action of (a) southwesterly (225°, 10 m/s), (b) southeasterly (115°, 8 m/s), (c) northerly (360°, 10 m/s), and (d) northwesterly (315°, 10 m/s) moderate winds obtained by integrating the velocity field with time step of 2 (a) and 4 (b-d) hours. Cross symbols show the points of tracer beginning; coordinate axes show the distance in km.

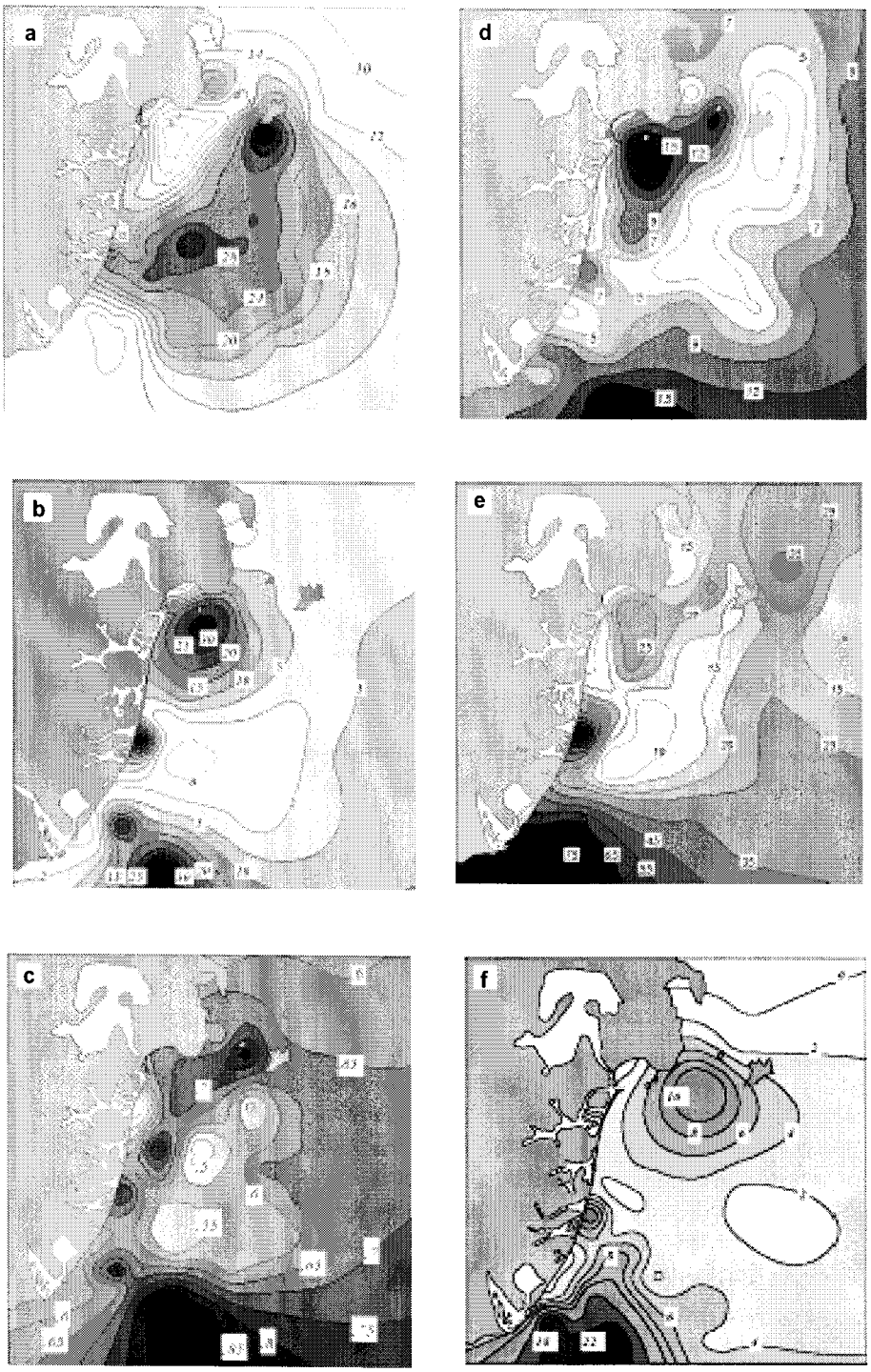

Fig. 7. Maps of the distribution of (a) mean granule size (mm), (b) percentage of <0.1-mm fraction (%), (c) entropy of granulometric distribution (arbitr. units), (d) total organic carbon (mg · g^{-1} of dried weight), (e) percentage of terrigenous organic carbon (%), and (f) lead (mkg · g^{-1} of dried weight) in the region studied.

the relatively low entropy of the granulometric distribution reveals the relative constancy of the sedimentation conditions. According to the results of the simulation for the most real wind situations, large velocities of steady current are obtained in this area.

5. Conclusions

The simulated wind-driven circulation in this study is satisfactorily agreed with the *in situ* data. Some features of the calculated patterns of currents are confirmed indirectly by the granulometric distribution of the seabed sediments, and by the location of accumulation zones of organic carbon and some pollutants. This model is not perfect and other additional studies might be required. Recent observations at moored buoy stations in the research area have shown that tidal fluctuations of current velocity are particularly noticeable in the vicinity of the sea floor near the continental slope. So, a multilayered (at least two layers) model should be tried for this region with emphasis on the tidal influence and the interaction with bottom relief features, particularly in the vicinity of the Tuman River mouth. Naturally, the main difficulty is to fit acceptable boundary conditions. Since we have no observations of the sea level or water transport along open boundaries, a measurement net of some moored buoy stations would be required. Now, we have done only a preliminary analysis of prevailing water pathways and transport of the suspended material. It is clear that the main source of bottom sediments in the Reserve is a solid discharge of Tuman River. So the most dangerous situation for the Far Eastern Federal Marine Reserve is the case of the southwesterly wind; even with the quite moderate wind forcing, the waters polluted by the run-off from Tuman River can attain the south section of the Marine Reserve within a diurnal period. A contamination process of the Reserve is supposed to be strongly increased by the construction of a large port in the Tuman River mouth.

Acknowledgements

We are very grateful to all anonymous reviewers for valuable remarks, encouraging us in continuation of work and for corrections of our English.

References

Beardsley, R.C. and D.B. Haidvogel. 1981. Model studies of the wind-driven transient circulation in the Middle Atlantic Bight. Part 1: Adiabatic boundary conditions. *J. Phys. Oceanogr.*, 11, 366-375.

Chapman, D.C. 1985. Numerical treatment of cross-shelf open boundaries in a barotropic coastal ocean model. *J. Phys. Oceanogr.*, 15, 1060-1075.

Duun-Christensen, J.T. 1975. The Representation of the surface pressure field in a two-dimensional hydrodynamic numerical model for the North Sea, the Skaggerrak, and Kattegat. *Deutche Hydrogr. Zeitschr.*, 28, 73-79.

Grigorieva, N.I. and A.V. Moshchenko. 1998. The study of water transport and hydrological conditions of the northward part of the region near the mouth of Tumannaya River. *Bulletin of the FEB RAS*, 1, 7-11 (In Russian).

Hansen, W. 1961. Hydrodynamic method applied to oceanographic problems. p. 25-30. In *Proc. Symp. Math. Hydrodyn. Meth. Phys. Oceanogr.*, Mitt. Inst. Meeresk. Univ., 1.

Henry, R.F. and N.S. Heaps. 1976. Storm surges in the southern Beaufort Sea. *J. Fish. Res. Board of Canada*, 33, 2362-2376.

Lastovetskiy, E.I. and L.P. Yakunin 1981. Hydrometeorological characteristics of the Far Eastern Marine Reserve. p. 18-33. In *Flowering Plants of the Far Eastern Marine Reservation*, FEB of USSR Academy of Sciences, Vladivostok (In Russian).

Menovshchikov, V.A. and A.V. Saveliev. 1989. Application of shallow water equations for calculation of currents on the shelf of Bering Sea during the storm situations. p. 77-85. In *Proc. FERHRI*, 39 (In Russian).

Moshchenko, A.V., N.S. Vanin, K.L. Feldman, and G.I. Yurasov. 1999a. Processes controlling the distribution of solid run-off of the Tumannaya River (Peter the Great Bay, Japan Sea). p. A193. In *IUGG99*. Birmingham, UK, Abstracts. XXII *In General* Assembly, IAPSO. P10/e/13-A5.

Moshchenko, A.V., N.S. Vanin, K.L. Feldman, and G.I. Yurasov. 1999b. Distribution of solid run-off and pollutants northward of Tumannaya River Mouth as a tracer of wind circulation (Peter the Great Bay, Sea of Japan). p.28-29. In *Global Change Studies in the Far East.*, Abstracts of workshop. Vladivostok, Russia.

Moshchenko, A.V., V.M. Shulkin, and T.S. Lishavskaya. 2001a. Factors controlling contaminant contents in the

coastal marine sediments of the region closed to the Tuman River mouth. *Geochemistry* (In press).

Moshchenko, A.V., N.S. Vanin, K.L. Feldman, and G.I. Yurasov. 2001b. Pattern of solid run-off and contaminants distribution in a basin northward of the Tumannaya River mouth as a tracer of wind currents (Peter the Great Bay, Sea of Japan). In *TEACOM Publication*, 5(In press).

Moshchenko, A.V., N.S. Vanin, and A.E. Lamykina. 2000. Bottom relief, sediments and hydrological conditions of the near-mouth area of Tuman River. p. 42-75. In *Ecological status and biota of the south-west part of Peter the Great Bay and Tuman River Mouth*. Collection of the papers. Vol. 1. Dalnauka, Vladivostok (In Russian).

Saveliev, A.V. 1989. Numerical modeling of the water dynamical condition forming by wind action on the shelf of Sakhalin eastern coast. p. 63-76. In *Proc. FERHRI*, 39 (In Russian).

Shulkin, V.M. and A.V. Moshchenko. 2000. Contaminant level and factors controlling contaminant contents in the bottom sediments of the region closed to the Tuman River mouth. p. 86-98. In *Ecological status and biota of the south-west part of the Peter the Great Bay and Tuman River Mouth*. Collection of the papers. Vol. 1. Dalnauka, Vladivostok (In Russian).

STATISTICA for Windows. 1996. StatSoft, Inc.

Volcinger, N.E. and R.V. Pyaskovskii. 1977. Theory of Shallow Water. Gidrometeoizdat., Leningrad. USSR (In Russian).

Received Jan. 13, 2000
Accepted Dec. 11, 2000